Geophysical and geochemical characterization of apatite mineralization on Mlindi Ring Structure

Chikondi Chisenga*[1], Hassan Steven Mdala[2], Annock Gabriel Chiona[2], & Denson Makwela[2]

[1] Malawi University of Science and Technology, P.O Box 5196, Limbe, Malawi.
[2] Geological Survey Department, P.O Box 27, Zomba, Malawi.

* Corresponding Author Email: cchisenga@must.ac.mw

Abstract

The geochemical and magnetic data of the Mlindi Ring Structure has been used to understand the full extent of the rare earth and base metal mineralization hosted in the apatite-rich meta-pyroxenite and other mafic to ultra-mafic rocks. Previous studies in Mlindi Ring Structure had only focused on understanding the agro-minerals economic potential from the apatite. However, this study's combination of geochemical and geophysical analyses of the Mlindi Ring Structure has identified it as a possible multi-commodity deposit. The Ring Structure contains considerable anomalous values for gold, zinc, nickel copper and rare earth elements. The mineralization of gold and base metals is found in almost all the lithologies but much higher in apatite-bearing meta-pyroxenite. On the other hand, rare earth elements are mostly associated with dark rocks i.e. meta-gabbro and meta-pyroxenite and less in silica-rich rocks like quartzofeldspathic gneisses. The soil thickness in Mlindi Ring Structure makes it difficult to understand the full mineralization in the rocks underneath it as very few outcrops are present. We combined the geochemical results with the aeromagnetic data analyses to estimate the full extent of the magnetic minerals which make the core of the Ring Structure using its susceptibility and depth estimates. Pyroxenite, meta-gabbro and biotite-rich mafic rocks show some apatite mineralization with a larger percentage in the meta-pyroxenite rather than the other mafic rocks.

Keywords: Magnetics, Malawi, meta-pyroxenite, Mlindi Ring Structure.

1. Introduction

The Mlindi Ring Structure is an alkaline ring complex, dated 495 ma, within the southern Malawi's basement complex, and is composed of a central mass of ultrabasic or syenitic rocks surrounded by annuli of inward dipping rings (Laval and Hottin, 1992). The structure was discovered in 1950 during a preliminary geological inspection of the aerial photographs

of Nyasaland (Bloomfield, 1965), which was thought to be a dome (Ashley, 1952), while other studies described it as an explosive vent linked to Chilwa alkaline province (Cooper, 1952). Detailed mapping of the Mlindi Ring Structure followed the discovery from aerial photography (Ashley, 1952a, 1952b; Morel, 1958; Bloomfield, 1957, 1959, 1960). The structure is one of the two non-carbonatite alkaline ring structures in Malawi with the rest comprising of carbonatites and agglomerates.

From an economic point of view, Mlindi ring structure is a source of agro minerals, mostly comprising of apatite bearing phosphate, occurring as flourapatite, and the presence of pottasium (Bloomfield, 1965). The apatite bearing biotite-pyroxenite rocks occur within the central part of the ring structure. Two areas with apatite rich residual soils were delineated within the central part of the structure, estimated at about 2.4 Mt with grades of 7% to 14% P_2O_5, (Chisale and Kaphwiyo, 1987). These apatite rich soils are probably the result of the weathering of the apatite rich meta-pyroxenite, which underlie the soil within the center of the ring structure. In addition to phosphates, there are considerable amounts of K-containing minerals within the area. The apatite rich soils thickness might reach the depth of 100 meters or more (Chisale and Kaphwiyo, 1987). To our knowledge, no detailed drilling program has ever been conducted in the area to understand the extent of the meta-pyroxenite underneath the thick layer of soil. However, a borehole of 27 meters deep was sunk around Butao village in 1956, which penetrated biotite-metapyroxenite (Bloomfield, and Garson, 1965). The information currently available only speculates on the extent of the mineralization in the apatite rich meta-pyroxenite within the ring structure.

Despite previous effort to understand the Mlindi ring structure, information is still scarce on the subsurface distribution and origin of the apatite bearing metapyroxenites. As such, the current study aims at provide the initial understanding of the surfaces structures and its relationships to the apatite mineralization. The previous geochemical study of the area, using 25 samples, was done to understand the mineralization pattern, with emphasis on the presence of Cr (40-1300 ppm), Cu (6-200 ppm), Ni (100-290 ppm) and Co (45-75 ppm) in meta-pyroxenite (Laval and Hottin, 1992). The study however, did not differentiate any trace-element trends. The availability of the high resolution magnetic data provides us with an opportunity to image the subsurface structures. Furthermore, 47 rock samples and 38 soil samples collected in the area provide a way to differentiate the zones of apatite rich meta-pyroxenite, by separating the meta-pyroxenite with the other high magnetic-rocks like meta-gabbro. The capability of apatite as an indicator of rare earth and trace elements mineralization in a multi-commodity deposit is well known (e.g. Belousova et al. 2002). The apatite presence can be a source of rare earth minerals especially the Lanthanides, which are associated with phosphates like fluorapatite, $Ca_{10}(PO_4)_6F_2$ (generally referred to as apatite), monazite, (Ce, LREE)PO_4, and, more rarely, xenotime (Y,HREE)PO_4 (Harlov et al. 2002). Thus, identification of the full extent of the apatite-hosting meta-pyroxenite could be an indicator of the economic potential of the ring structure.

2. Geological setting

2.1. Regional geology

The Mlindi Ring Structure is located within the crystalline Basement Complex rocks, which are referred to as the "Malawi Basement Complex rocks". These rocks are of Precambrian to Palaeozoic in age, which consist of gneisses and granites. They have undergone a medium to high grade metamorphism and a prolonged structural and metamorphic history, which was dominated by orogenic movements, faulting, rifting and formation of the Malawi Rift Valley (Carter and Bennet, 1973). The Mlindi Ring Structure is in proximity to the Chilwa Alkaline Province of Cretaceous to Jurassic age, which composed of roughly circular quartz syenite bodies with nepheline syenite intrusions and alkaline granite. This province was an area of alkaline magmatism from the Jurassic to the Early Cretaceous, and was probably emplaced before the Early Cretaceous carbonatite complexes, such as the Kangankunde carbonatite. The Mlindi ring Complex intruded the gneissic basement, which was formed during the Ordovician period. It was emplaced during a period of magmatic and orogenic calm after the last Pan-African events and before the widespread Karroo tectonism. Occurrence of ring structures has been documented within the southern part of Malawi (see Figure. 1), which among them include the Mlindi, Chipilanje-Little Michiru, Chingale and Ntonya (Bloomfield, 1965).
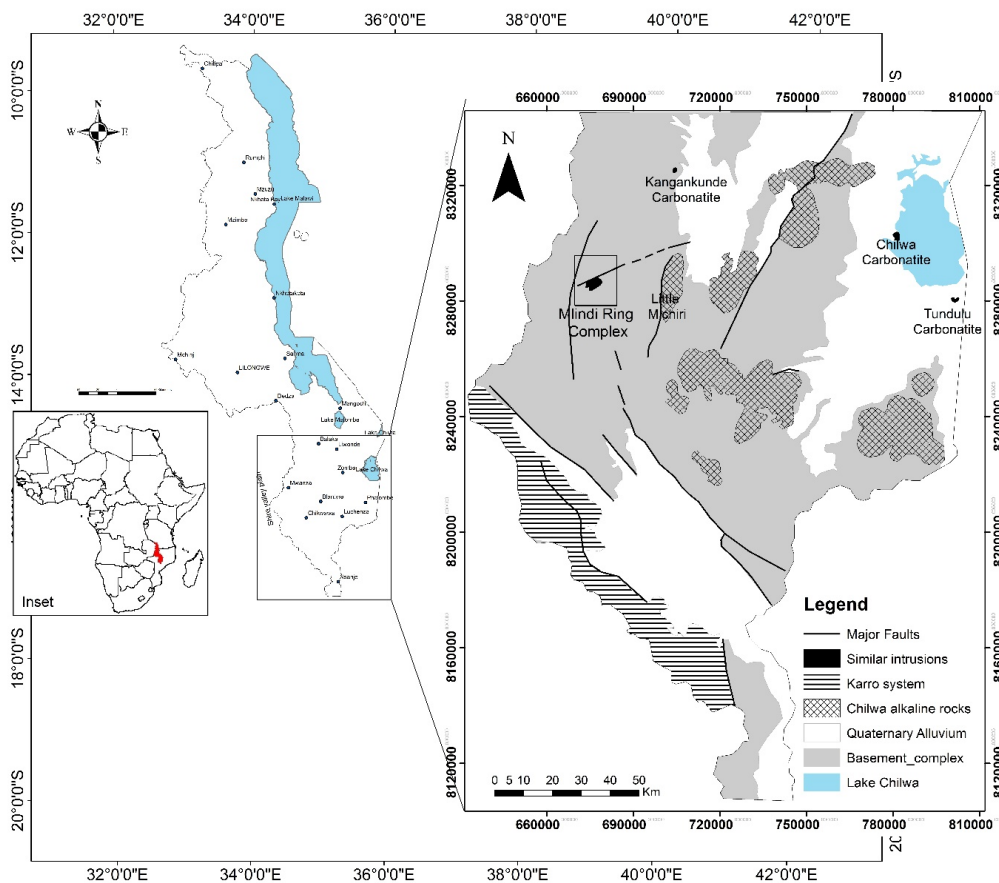
Figure 1: The geological sketch of regional geology of southern Malawi: showing location of Mlindi ring structure and the location of the study area in relation to the African continent.

2.2. Local Geology

The Mlindi Ring Complex contains progressive rings of biotite-metapyroxenite, meta-gabbronorite to syeno-meta-gabbro, meta-gabbro-diorite and syenite from the center outwards (see Figure. 2). The ring complex is cut by numerous dykes and veins of pegmatite, micro-syenite, solvsbergites and lamprophyre. The ring structure is surrounded by the Precambrian paragneisses basement rocks comprising semi-pelitic hornblende-biotite gneisses with subsidiary bands of quartzofeldspathic gneiss, dolomitic marble, schist as well as garnetiferous and graphitic types (Morel, 1958; Bloomfield, 1960). The ring structure also consists of basic and ultrabasic rocks associated with syenite (Perthosite), which are

mainly restricted in the central part with some smaller marginal Structures (Bloomfield, 1960).

The apatite bearing meta-pyroxenite rocks, which are associated with meta-gabbro and biotite, occupy an area of about five square kilometers around Ligowe Village and are limited to this locality. The lithologies give rise to a low relief characterized by a slick micaceous soil, which appears to be highly suitable for agricultural purposes rich in apatite. Small knolls of ultrabasic rocks stand out above the alluvial ground (Bloomfield, 1965). To the east of Neno road, about two kilometers south of Ligowe, there are some exposures of pyroxenite. In one locality, a small cliff, shows a mass of very course biotite-rich pyroxenite containing visible pale – green apatite clean cut by six inch wide finer- grained syenogabbro dykes trending at N 7º E (Bloomfield, 1960). Several small outcrops of pyroxene-perthosite are seen within the ring structures with the largest forming Liwone Hill to the western side of Ligowe Village.

3. Data

3.1. Aeromagnetic data

We used aeromagnetic data obtained from Geological Survey of Malawi. The data was collected during the 2013 – 2014 high resolution geophysical survey of Malawi by Sanders Geophysics Limited, which was jointly funded by the European Union and the World Bank. The survey line spacing was 250 m with a 5000 tie lines flying at altitude of 80 +-20 m. The traverse direction was in a NE-SW while control lines were in a NW-SW direction (Bates and Mechennef, 2013b, 2013a). The ring structure shows a circular dipole anomaly with value greater than 200nT. However, the surrounding areas show low magnetic anomaly, which is also noticed at the center of the ring structure. Mlindi hill in the south-eastern part of the study area indicates high magnetic values between 150nT and 300nT. The highest recorded amplitude of 1869nT is located within the center of the Mlindi Ring Structure's meta-pyroxenite rocks hosting the apatite.
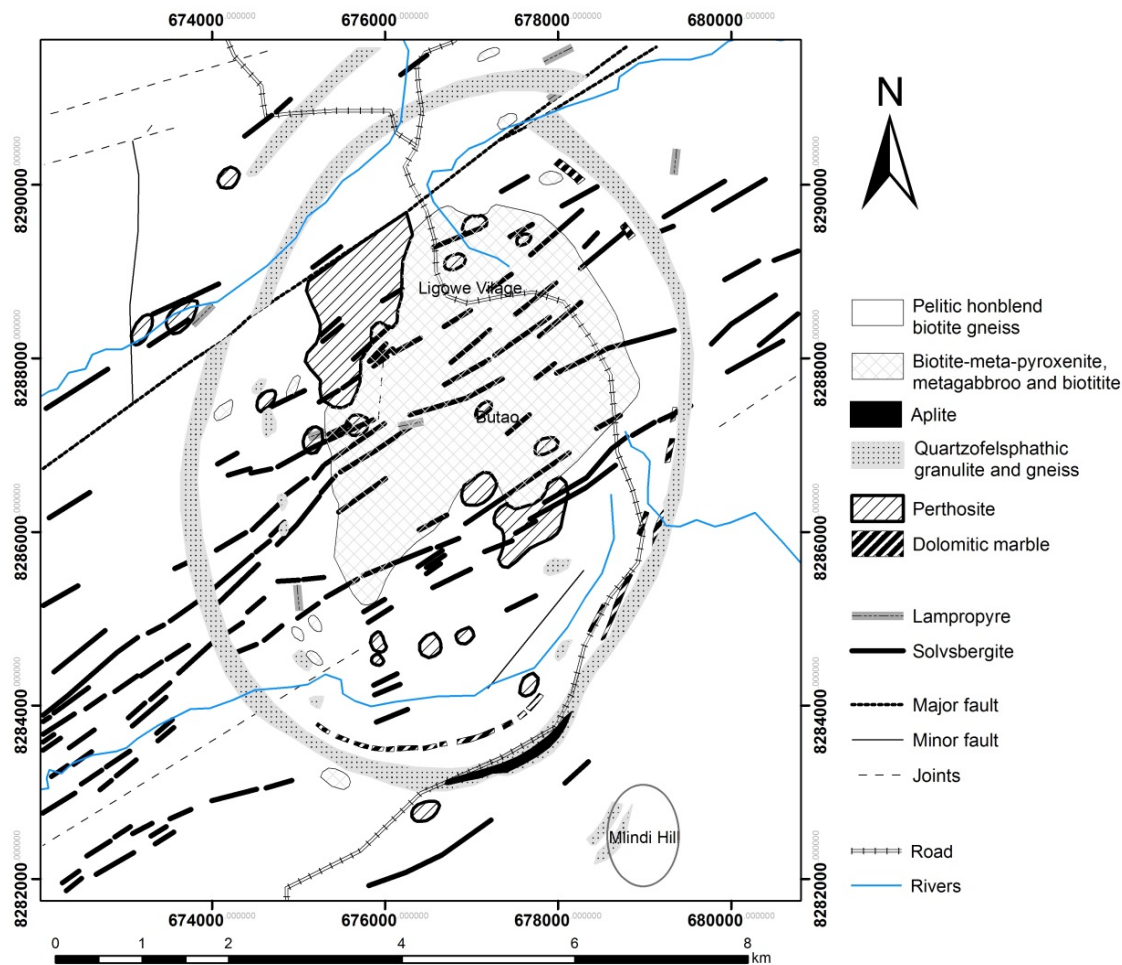
Figure 2: The Geology of Mlindi Ring Structure after Bloomfield, (1957, 1959); and Morel, (1958).

3.2. Geochemical data

We also used soil and rock samples collected from meta-pyroxenite outcrops in the Mlindi Ring Structure and the meta-gabbro, quartzofeldspathic granulites and biotite gneiss in the surrounding areas. Initially, remote sensing was used to map the extent and alteration area of the Mlindi Ring Structure. Purposive sampling method was conducted to cover areas which were passable and the terrain was not difficult with visible outcrops within this area selected by remote sensing techniques. The sampling of fresh rock exposures and soil was done randomly, which cover the entire rock units within the Mlindi Ring Structure. The depth of at least 30 cm was preferred to avoid humus in soil sampling from agricultural residuals. Half a kilogram of a sample was collected for each location. A total of 51 locations were visited with 47 rock samples and 38 soil samples collected within an area of

~65 km² (Figure 3). Of these, 21 of the locations were within the center of the Ring Structure, in the meta-pyroxenite. We targeted rare earth elements and trace elements in the meta-pyroxenite hosting apatite at the Mlindi Ring Structure.
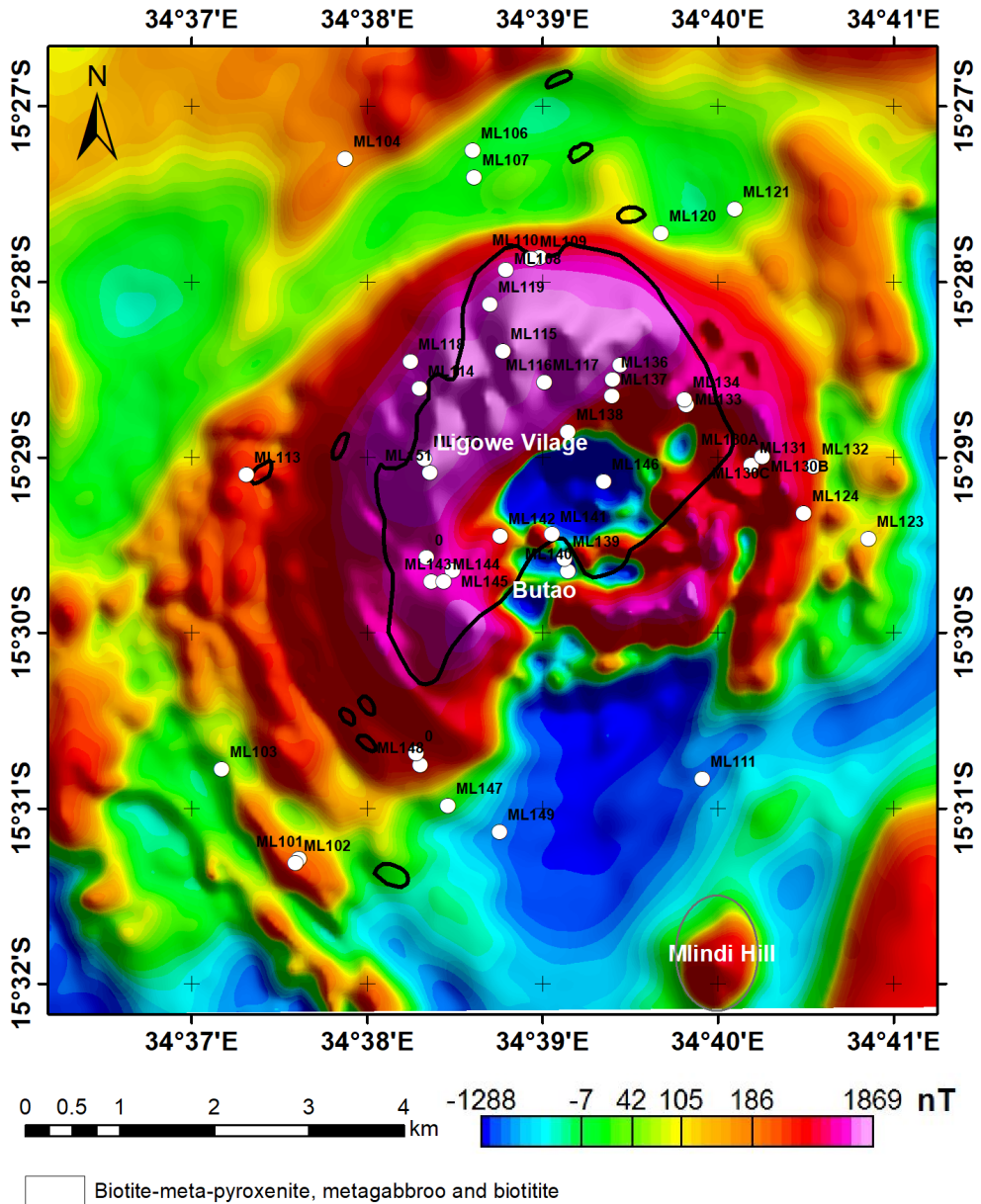

Figure 3: Data used for the study: Total Magnetic Intensity map (TMI) with geochemical sampling point location and extent of meta-pyroxenite based on geological data

4. Methods

4.1. Reduce to pole and apparent susceptibility

Magnetic anomalies are affected by the dipolar effect due to the magnetic inclination of the earth's magnetic field. The anomalies are reduced to pole to avoid this effect, which make the magnetic anomaly to lie directly above the magnetic source body and geology (Jachens and Blakely, 1986). We then used reduce to pole data to calculate the apparent susceptibility. This differentiates the signal from meta-pyroxenite and other mafic apatite-bearing rocks in the Mlindi Structure to other non-apatite bearing magnetic rocks. The apparent susceptibility calculation models the continuous magnetic signal to the approximation values of susceptibility of rocks in the ground, which reduce anomaly overlaps as regional field is removed and data is downward continued closer to source body/geology (Letros et al, 1983; Ranganai and Ebinger, 2008). The apparent susceptibility was calculated using the magnetic inclination value of -48.85°, magnetic declination of -4.904°, total magnetic field value of 31750.8nT and downward continued the data to depth of 100, 150 and 200 meters (100 meters being the minimum inferred soil thickness in the center of the Mlindi Ring Structure (Kaphwiyo and Chisale, 1987). The calculated susceptibility values were converted to SI from electromagnetic units using a factor of 12.57 or $4\prod$ or $(4\prod)^2$ x 10^{-7} (Clark and Emerson, 1991) with $\prod$ value of 3.14.

4.2. Euler deconvolution

We estimated the possible depth estimate of the apatite bearing meta-pyroxenite using the Euler deconvolution technique. We used this approach as it automatically determines the depth of magnetic source bodies in the data without the use of a prior data, by solving Euler equation (Mushayandebvu et al., 2004; Reid et al., 1990). Due to the limited geological information about the depth of the meta-pyroxenite and other apatite bearing rocks in the Mlindi Ring Structure, the technique was ideal in determining the depth and boundary of apatite bearing meta-pyroxenite. However, the results from this technique are in form of points, e.g. Euler solutions when using Euler deconvolution method (Reid et al.,1990). This brings challenges in geological interpretation, which renders our results far more difficult to interpret. We applied the Euler deconvolution on the analytical signal to reduce the number of Euler solutions, which removed extraneous depth estimates. The magnetic grid was expanded by 20% to avoid the tapering effect on the edges. Three derivatives were calculated from the magnetic grid, a derivative in the x direction, y direction and Z directions. The convolution is sensitive to the shape of the anomaly and the absolute depth and not the total magnetic value of the source bodies (Li and Morozov, 2007). Thus, the shape, orientation and geometry of the magnetic source were controlled by a parameter called structural index (Reid et al., 2003). A structual index of 3 was used to identify dome like structures for meta-pyroxenite.

4.3. Geochemical analysis

We analyzed the elemental concentration in the rock and soil samples using the Thermo Scientific Portable X-Ray Fluorescence (XRF) analyzer. The XL3t 950 XRF model has a maximum scatter net dose rate of 100 micro rem and a sampling window of 5cm. The results from the measurements are net values above background values. It should be noted that portable XRF are prone to errors compared with the laboratory XRF machine. Background values return the results of "ND"; not distinguishable or detectable. Before analysis, we calibrated the XRF against the soil samples that came with the machine, whose results were almost similar with uncertainty range within 5%. We used the geochemical results to determine the geochemical signature of Mlindi Ring Structure as a potential rare earth and trace element deposit, using the presence of apatite as an indicator. Due to the limitation of the analysis window for the XRF, 10 random points were measured on each of the samples and then averaged. Despite that, an uneven distribution of elements in the sample is not fully dealt with, but multiple measurements remove the biasness of a point in the measurement. Another limitation of the handheld XRF is its failure to detect Na. Some studies have shown that igneous rock have a specifical K/Na ratio (Iddings, 1898; Alva-Valdivia *et al.*, 2001; Broughm *et al.*, 2017). We used the K_2O/ Na_2O ratio for the geochemical data by Laval and Hottin, (1992) to calculate for the Na_2O in our analyzed samples.

5. Results and discussion

5.1. Field observations

We discuss the relationship between lithology and structures in the Mlindi Ring Structure based on the field observation during the field work. Meta-pyroxenite is mostly covered by the apatite rich soils with few outcrops noticed at the center of the ring structure. Most of the outcrops are course grained minerals. However, in some localities medium grained meta-pyroxenite were observed. Pale to green apatite was visible in course grained biotite-meta-pyroxenite. We sampled each meta-pyroxenite locality systematically to get a representative rock chip per outcrop. In some instances, weathered rocks and cross-cutting veins were also sampled. We identified pyroxenes, biotite and K-feldspar, with rare cases of quartz and muscovite in the meta-pyroxenite.

Quartzofeldspathic gneiss and granulite forms a ring-like dyke around the inner meta-pyroxenite, which changes from granulite to gneiss at different localities along its course. Coarse grained lithology was observed, which was highly weathered in some localities. The presence of secondary alteration is visible in the quartzofeldspathic gneisses. In some localities, there was presence of fractures with greenish minerals, possibly epidote or chlorite. Besides quartz and feldspar, hornblende and muscovite were also present. In some localities, feldspar content exceeded 60% of the rock mineral composition.

In Mlindi Ring Structure, Perthosite/perthitic gneiss occurrences are associated with meta-pyroxenite. Massive coarse grained Perthosite are located within the center of the ring structure extruding the meta-pyroxenite. No fine grained Perthosite was observed or sampled in the area. Less abundant are the mesocratic rocks associated with Perthosite with >55% quartz and >30% hornblende. In some areas, Perthosites are characterized by mafic dykes/xenoliths cutting across them. These dykes are characterized by a pale to greenish mineral, which was probably apatite.

A number of minor lithological occurrences, aplite, meta-gabbro, micro-syenite, solvsbergites and syenite dykes as well as lamprophyre, are also found in the study area. Aplite occurs in a single locality as a leucocratic medium to coarse grained dyke. It shows abundance of plagioclase feldspar with quartz, hornblende and biotite. Meta-gabbro exists as small outcrops with pegmatite/quartz veins running through them. The veins and dykes of micro-syenite, lamprophyre and solvsbergites are also found in many localities within the study area.

5.2. Magnetic susceptibility

Magnetic anomalies in the Mlindi Ring Structure are attributed to the dark minerals, which contain iron and magnesium (Fe-Mg), mainly from meta-pyroxenite and meta-gabbro. Magnetite mineralization during regional metamorphism of the area also contributed to this magnetic anomaly. Field observations indicate presence of big crystals of mineralized magnetite in the quartzofeldspathic granulite and gneiss. However, the calculated magnetic susceptibility of quartzofeldspathic granulites and gneiss is relatively small on the surface (Table 1). At depth, the susceptibility is higher in quartzofeldspathic granulites and gneiss, despite no clear explanation of such elevated values. The trend is also noticed in the gneisses, which form the Basement Complex of Mlindi Ring Structure. It is assumed here that the elevated susceptibility values at depth within the quartzofeldspathic granulites and gneisses may be attributed to quartzofeldspathic – metapyroxenite contact at depth.

The susceptibility of Perthosite is considerably higher compared with other silica rich rocks in Mlindi Ring Structure. The field observations and susceptibility of rocks calculated from magnetic data indicates that the anomaly at the center of the ring structure emanate from meta-pyroxenite and meta-gabbro, with little influence from other lithologies (Figure 4). The coverage of apatite rich soils conceals the extent of meta-gabbro intrusion, even close to the surface. Meta-gabbro is visible in only one location with 14 visible outcrops of meta-pyroxenite. Thus, we suggest that to greater extent, magnetic anomaly in the center of Mlindi Ring Structure is caused by meta-pyroxenite and to lesser degree meta-gabbro.
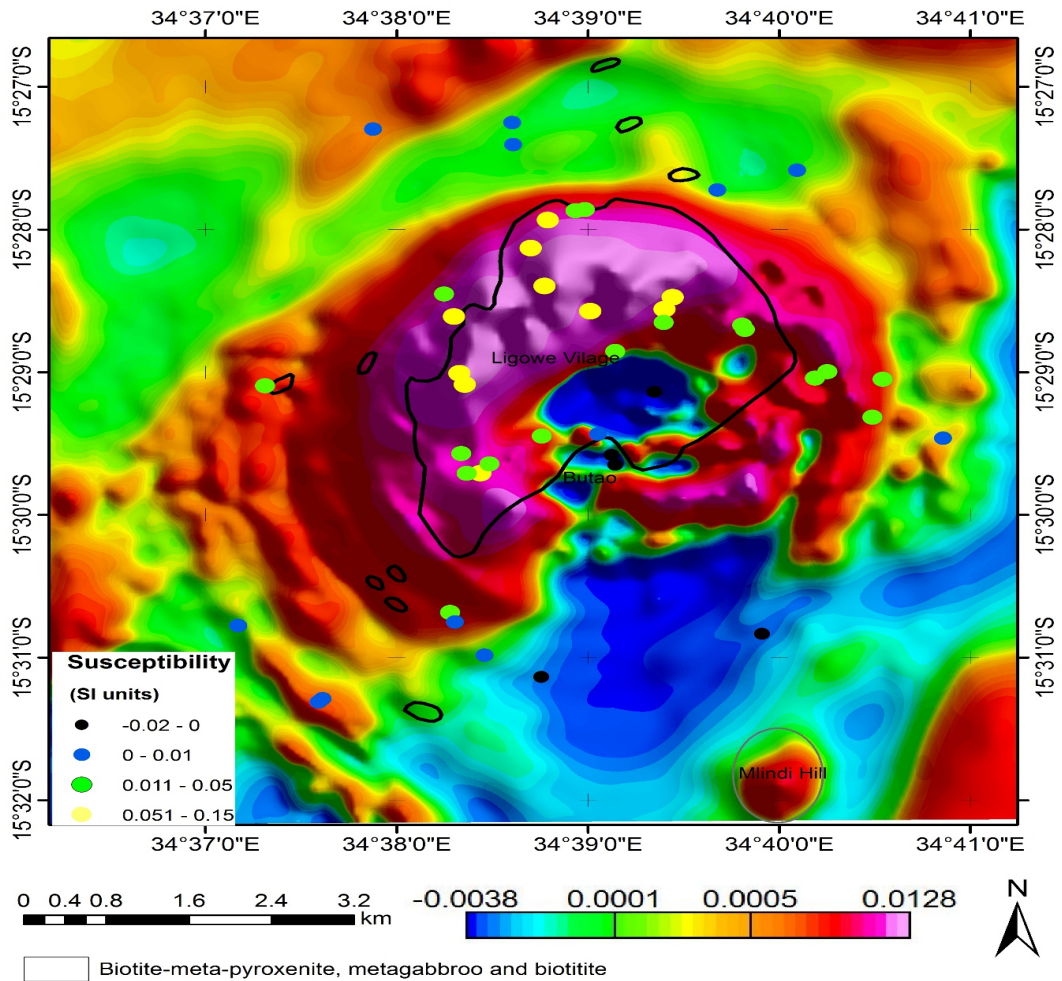
Figure 4: Apparent susceptibility map indicating geochemical data points in which magnetic susceptibility was constrained and the geological extent of meta-pyroxenite geology.

5.3 Depth estimates

The depth estimates of the Mlindi Ring Structure provide much information to determine the magnetic source of most of the anomalies. Magnetic source body range from the depth of 50 m to less than 250 m.

The northern part of the meta-pyroxenite, which show high magnetic anomaly, is well resolved from the Euler deconvolution. This is in agreement with susceptibility values which shows high magnetic values at greater than 50 m depth (Figure 4 and Table 1). However, the possible magnetic source indicates magnetic source depth of less than 50 m,

which agrees with considerable outcrops of meta-pyroxenite on the surface in this region. The second suggestion indicates that at depth, the magnetic values are higher in the center of the Ring Structure around 150 m to 250 m, indicating a possible inward dipping lithologies on a contact between them. From 150 m going downwards, there is no indication of magnetic minerals for most of the meta-pyroxenite outcrop. This indicate that the top of the magnetic signals is shallower in the meta-pyroxenite regions. At greater than 250 m depth, there is no indication of magnetic values; we propose two assumptions here (i) this may imply that the meta-pyroxenite mineralization doesn't reach this far, and (ii) this may be attributed to the effect of magnetic signal decay as observed by Lee et al. (2010) and Sadek et al. (1984); which means that at depths > 250 m the magnetic signal from the meta-pyroxenite mineralization decays before reaching the sensor. Other known magnetic region, e.g. the Mlindi Hill, also show shallow source of magnetics. Comparison of some few meta-pyroxenite outcrops and meta-gabbro indicates deeper sources and its susceptibility increase exponentially (Table 1).

5.4 Whole rock geochemistry

The major petrochemistry analysis of the Mlindi Structure was done to understand the environment of apatite mineralization within each lithology. The results show that the major source of phosphate (P_2O_5) and calcium oxide (CaO) in the Mlindi Ring Structure is the apatite (Ca_{10} (PO_4)$6F_2$). The chemical analysis of meta-pyroxenite in the Ring Structure indicates the signature of basic rocks (Figure 6).

Table 1: Magnetic susceptibility of major rocks in Mlindi Ring Structure with different upward continued depth

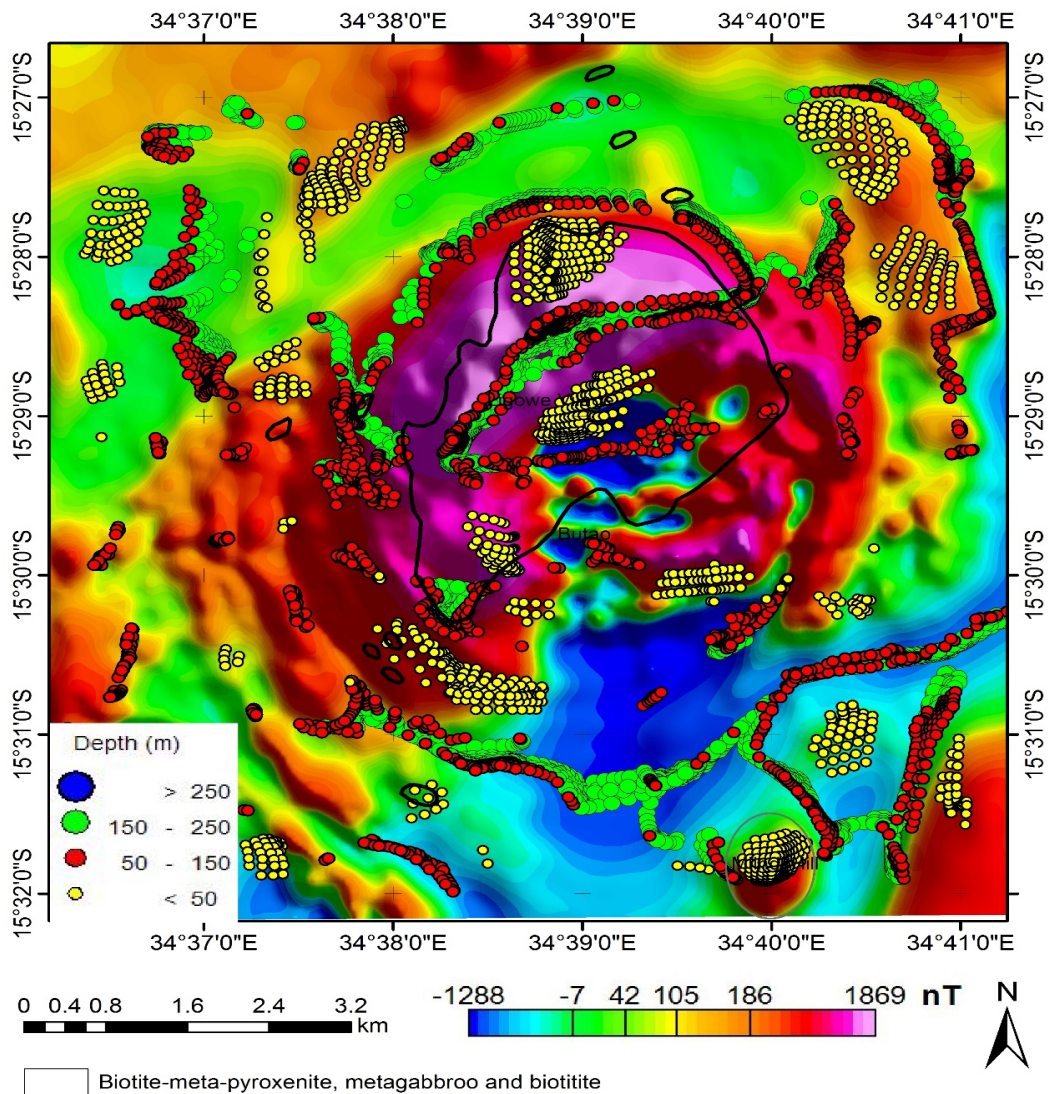| Rock units susceptibility	at surface		100 m		150 m		200 m	
	Range	average	range	average	range	average	range	average
Meta-pyroxenite	-0.02 – 0.15	**0.039**	-0.02 - 0.35	**0.05**	-0.08 - 0.9	**0.09**	-1.6 – 7.67	**0.6**
Quartzofeldspathic	-0.005 – 0.087	**0.017**	-0.007 – 0.08	**0.014**	-	**-**	-	**-**
Perthosite	-0.01 – 0.098	**0.033**	-0.05 – 0.16	**0.04**	-	**-**	-	**-**
meta-gabbro	0.008	**0.008**	0.015	**0.015**	0.024	**0.024**	0.119	**0.119**
Gneisses-basement	0 – 0.01	**0.002**	0 – 0.01	**0.002**	-	**-**	-	**-**

Figure 5: Depth estimates of magnetic body over RTP map for a structure index of 3 representing sphere like Structures.
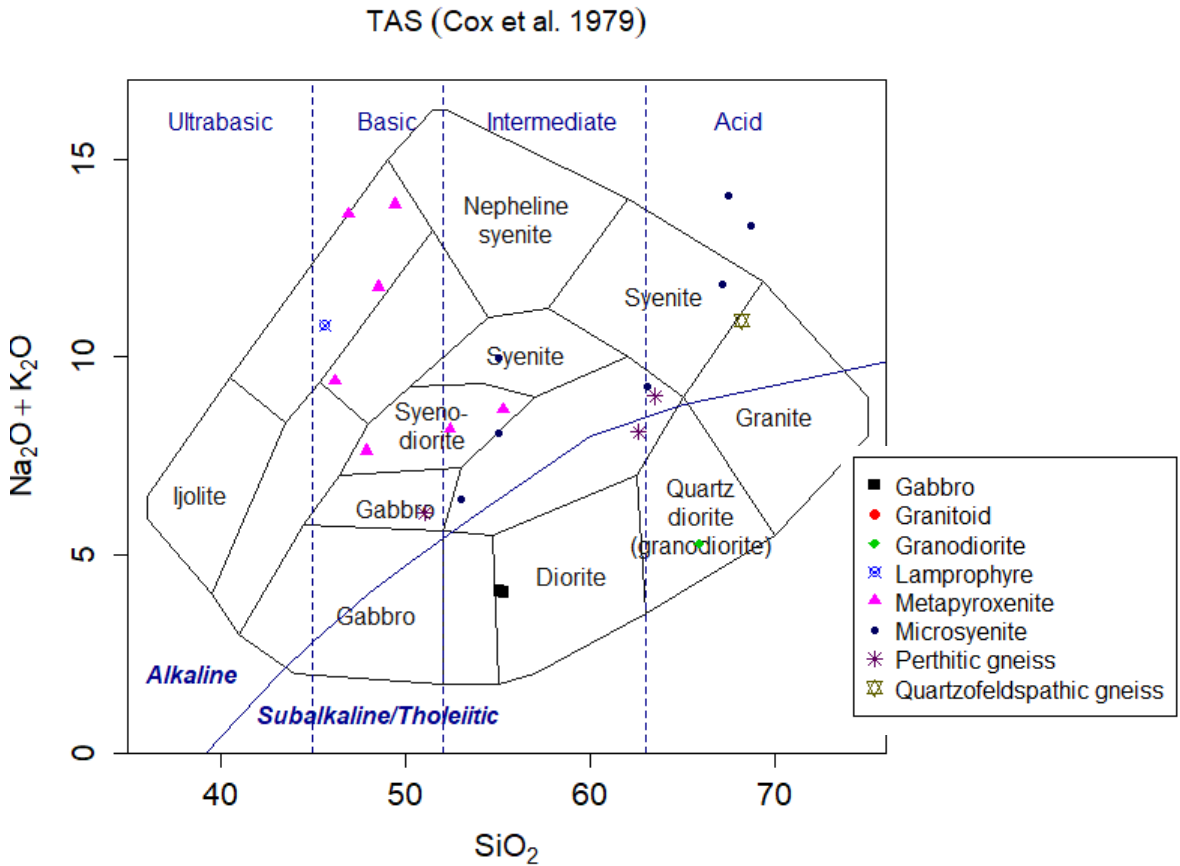
Figure 6: Classification of the rocks in the Mlindi area based on Total Silica Alkalis |(TAS) classification after Cox et al (1979).

The results suggests that the signature contains a considerable amount of iron and magnesium. Iron oxide (Fe_2O_3) ranges from 4.9 to 11.7 % while MgO goes up to 12.9 %. The presence of apatite in the meta-pyroxenite can be seen in the field samples. This is also shown in the petrochemical analysis results from the presence of phosphate and calcium oxides. The results also indicate that there is a direct relationship between P_2O_5 and CaO in the meta-pyroxenite. No apatite is present in other rock units as compared to meta-pyroxenite, which suggest that their formation was during early stages of the Bowens reaction series. Each of the localities of meta-pyroxenite from the analyzed samples shows wide variation of apatite and phosphate concentration. This indicates a long crystallization period or different mineralogical composition of the possible feeder pipes. It is also indicated in grain size difference for meta-pyroxenite within the Mlindi Ring Structure.

Course-grained meta-pyroxenite have more phosphate and calcium content than fine-grained outcrops.

The silica content in all rock units indicates a lot of variation within each lithology such that a clear pattern of relationship between apatite bearing meta-pyroxenite and other rock units is clear. The SiO_2 content is higher in quartzofeldspathic granulites and gneisses. It shows up to 92% in one locality and a minimum of 42%. In Perthosite, one location shows a higher percentage of silica of about 67%. Both Perthosite and quartzofeldspathic granulites show low or no values of phosphate. Calcium is present in small quantities. Those locations that show presence of calcium do not show phosphate and vice versa. The presence of these elements indicates normal earth elemental distributions above background values and not mineralization of apatite. However, cross-cutting relationship indicates presence of meta-pyroxenite in some Perthosite. These locations show presence of phosphate, which is of autochthonous origin in the Perthosite. The coarse grains and absence of apatite in Perthosite and quartzofeldspathic rocks indicate late and long crystallization period. We suggest that there was probably syngeneic crystallization of apatite with the dark minerals in meta-pyroxenite and meta-gabbro. The presence of TiO_2 in all the lithologies, which is evenly distributed, also indicates that the parental melt was not a barren residual magma. Despite that, the titanium oxide is higher in meta-pyroxenite compared with other major rock units in Mlindi Ring Structure. Figure 7 shows the summary of the SiO_2 vs oxide variation diagrams for the various rocks. Metapyroxinites largely show high K_2O, NaO and P_2O_5 contents. Different clusters of the rocks can be noted although Metapyroxinites are variable and do not seem to show pattern.
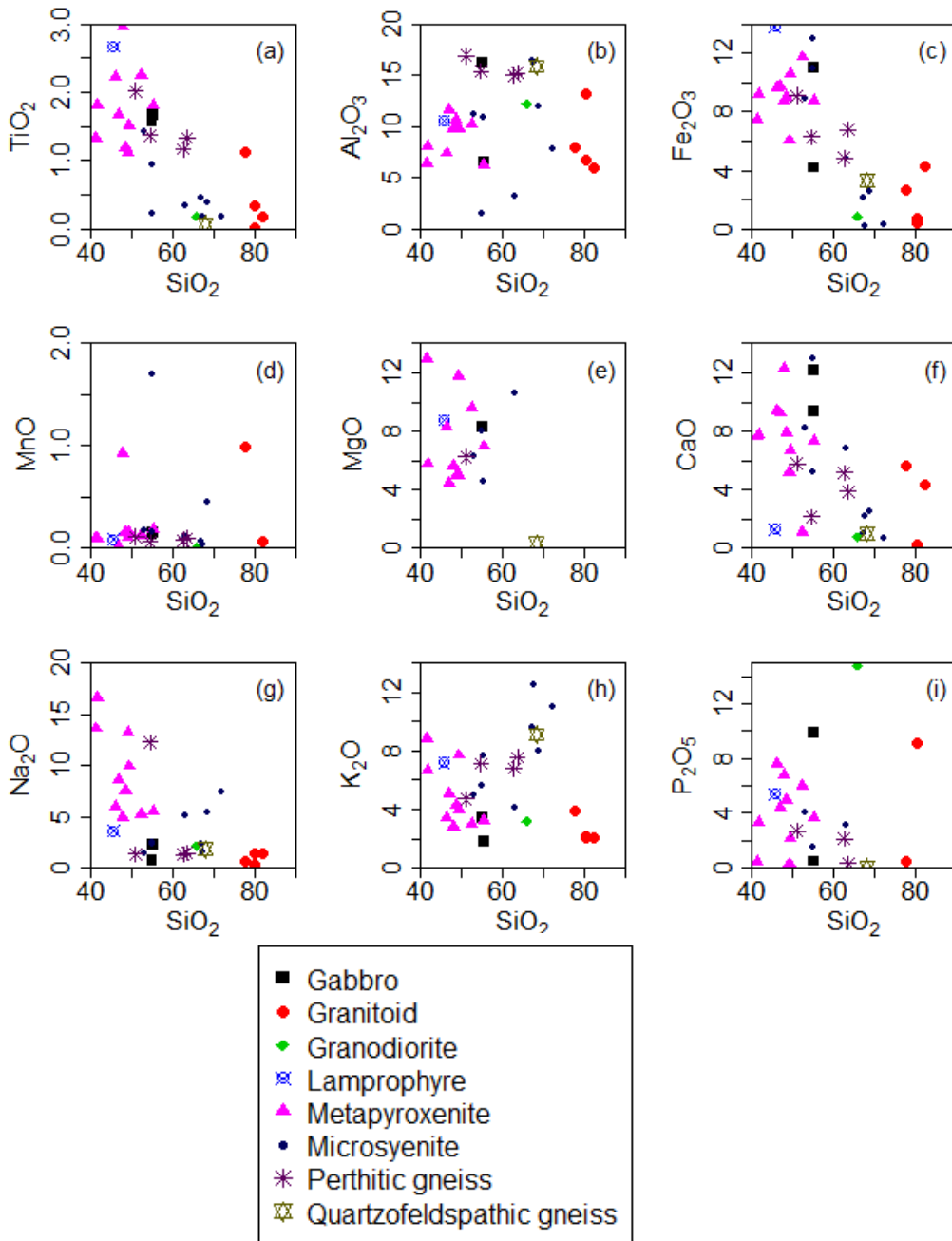
Figure 7: Oxide to oxide (wt.%) variation diagrams for different rocks in the Mlindi ring structure

5.5 Trace elements geochemistry

The trace elements geochemistry results are based on the XRF analysis. The analysis however, did not find any heavy rare earth minerals in Mlindi Ring Structure (Table 2), although Yttrium, which is mostly associated with heavy rare earth minerals, is present (Szumigala and Weldon, 2011, Fleischer, 1965; Innocenzi, Michelis, Kopacek, and Vegliò, 2014; Kanazawa and Kamitani, 2006; Wang, Pranolo, and Cheng, 2011).

The geochemical data for rocks with high P also have high K content as well as Pr and Nd content. This suggests that potential of some REEs in these rocks could be associated with potassic alteration. In addition, high magnetic response is also observed in these apatite-rich rocks (Sections 5.2 and 5.3). One of the reasons for the magnetic response could be due to the high titan content, which is also observed in these rocks apatite rich rocks. For example, both Figures 8 and 9 show that rocks with high P and K are associated with high Ti. Furthermore, our results show that hematite, rutile and ilmenite, which are all magnetic, are also present in most rocks that contains apatite. Therefore, we propose that the geochemical justification behind the high magnetic response in the apatite rich meta-pyroxenite and to lesser extent meta-gabbro is due to the presence of these minerals.
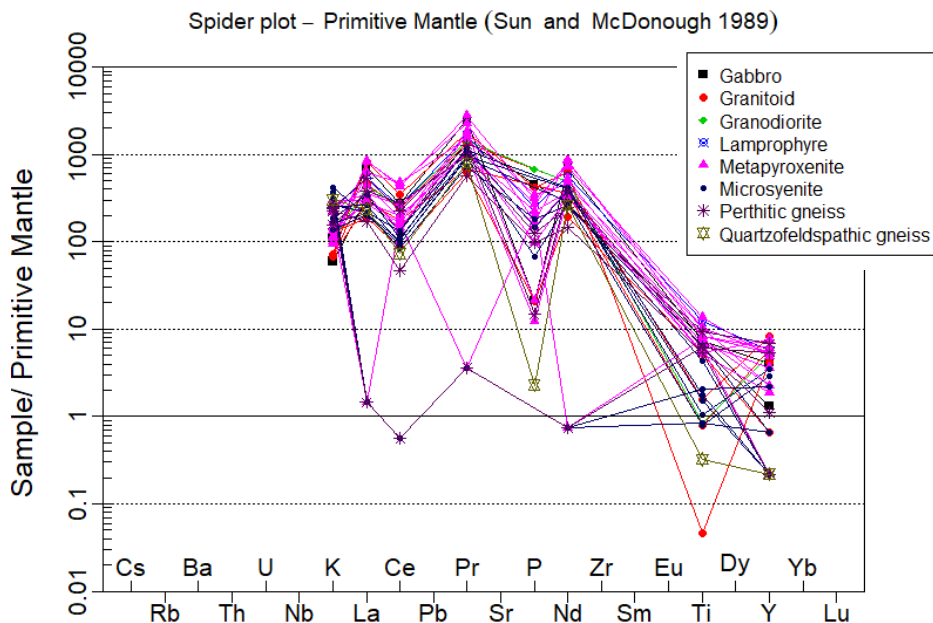

Figure 8: Spider diagram for the trace elements of rock samples of the Mlindi area normalized to the primitive mantle crust (after Sun and Mc Donough (1989).
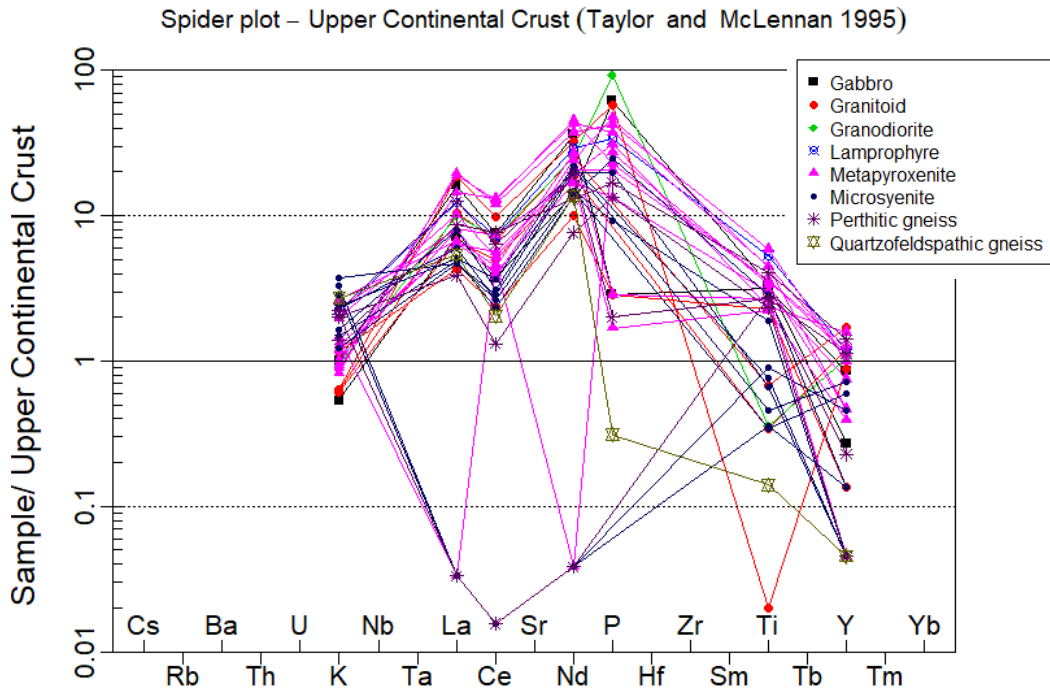
Figure 9: Spider diagram for the trace elements of rock samples of the Mlindi area normalized to the primitive mantle crust (after Taylor and McDonough (1995).

The geochemical analyses have shown that apatite is more associated with light rare earth elements than the heavy rare earth elements. The Mlindi Ring Structure is further associated with other key base metals, as shown in Table 2. As such, the Ring complex has more potential for light rare earth elements and economic minerals such as gold, nickel, and chromite. However, the potential for heavy rare earth elements cannot be ruled out at this stage considering the considerable presence of scandium and Yttrium within the area.

Table 2: Summary of Descriptive statistics for the rare earths and other key economic minerals in Mlindi area in ppm

Statistic	Sc	La	Ce	Pr	Nd	Y	Au	P	Cr	Mn	Ni	Cu	Zn
Mean	115.8	245.2	321.9	318.7	522.5	18.8	5.0	8,636.6	80.8	2,066.2	128.5	44.0	67.1
Median	26.0	202.5	286.3	287.9	506.9	16.5	3.0	200.0	36.6	770.0	98.0	37.0	71.3
Standard Dev.	430.4	153.8	212.5	195.9	311.1	21.4	11.6	14,268.8	142.7	7,842.4	131.9	38.1	49.0
Sample Variance	185,242.7	23,666.0	45,149.2	38,372.0	96,787.2	459.7	134.2	203,599,378	20,363.5	61,503,355.7	17,398.4	1,452.5	2,403.3
Skewness	6.2	0.5	0.7	0.4	0.5	3.6	5.6	2.2	4.0	6.3	2.2	1.4	0.3
Range	2,776.5	587.8	839.5	769.8	1,257.7	130.7	74.0	64,700.0	900.0	50,888.6	650.5	157.7	161.3
Minimum	0	0	0	0	0	0	0	0	0	0	20.0	2.0	2.0
Maximum	2,769.5	587.8	839.5	769.8	1,257.7	130.7	74.0	64,700.0	835.0	50,888.6	670.5	159.7	163.3
Sum	4,746.2	10,053.5	13,197.4	13,066.5	21,423.1	772.7	203.5	354,100.0	3,313.7	84,715.0	5,266.8	1,805.5	2,750.6
Count	41	41	41	41	41	41	41	41	41	41	41	41	41
Confidence Level(95.0%)	135.9	48.6	67.1	61.8	98.2	6.8	3.7	4,503.8	45.0	2,475.4	41.6	12.0	15.5

Table 3: Correlation matrix for rare earths and other key economic minerals in Mlindi Ring Structure

	Sc	La	Ce	Pr	Nd	Au	P	Y	Cr	Mn	Ni	Cu	Zn
Sc	1												
La	-0.07	1											
Ce	-0.20	0.86	1										
Pr	-0.19	0.89	0.74	1									
Nd	-0.18	0.89	0.84	0.92	1								
Au	0.11	0.12	0.10	0.06	0.08	1							
P	-0.13	0.03	0.10	0.09	0.03	0.18	1						
Y	0.18	0.47	0.45	0.44	0.53	0.05	-0.12	1					
Cr	0.85	0.00	-0.05	-0.15	-0.11	0.04	-0.19	0.03	1				
Mn	0.98	-0.11	-0.22	-0.25	-0.24	0.07	-0.10	0.05	0.87	1			
Ni	-0.09	0.41	0.45	0.33	0.39	0.31	0.06	0.11	0.06	-0.08	1		
Cu	0.14	0.47	0.44	0.30	0.34	0.44	0.05	0.22	0.21	0.14	0.69	1	
Zn	-0.20	0.30	0.49	0.23	0.34	0.19	0.03	0.19	0.09	-0.16	0.51	0.52	1

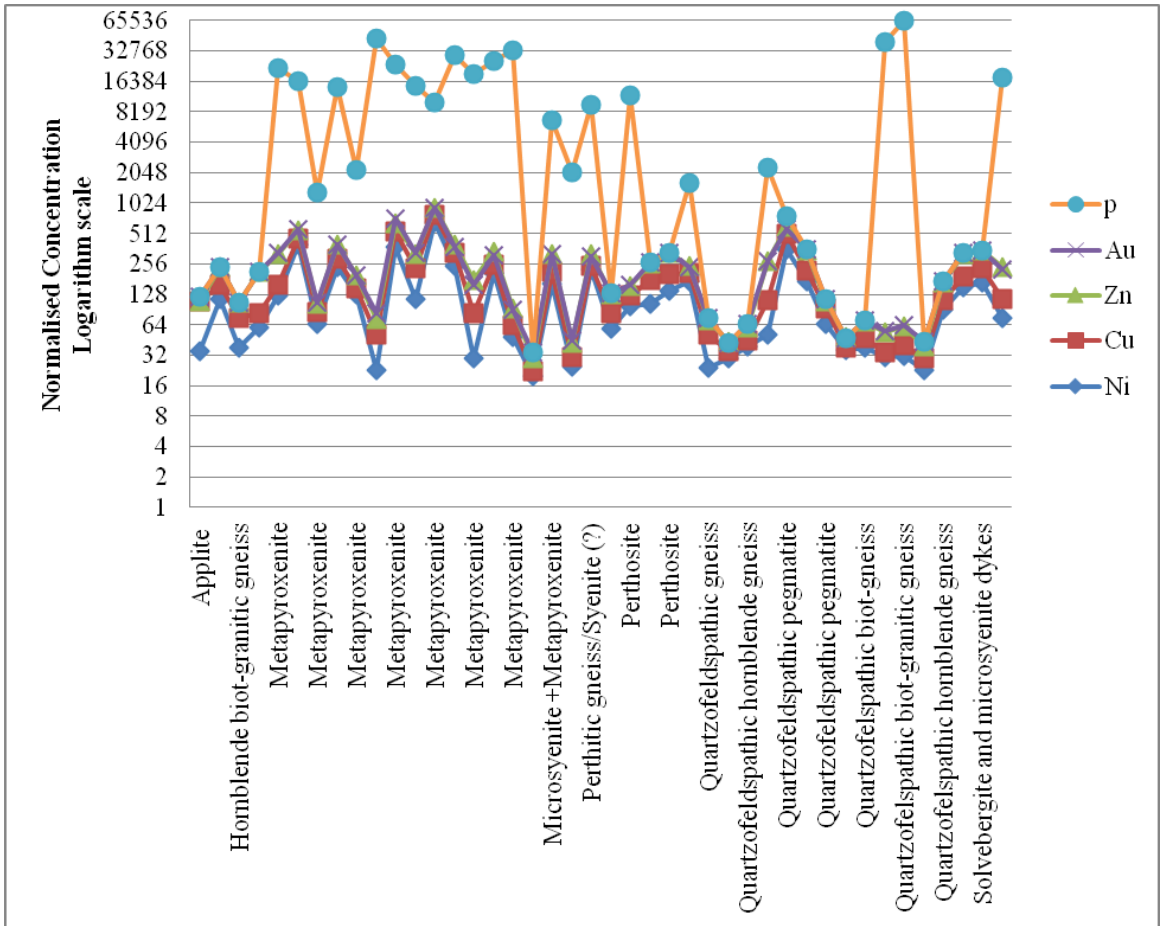| Key |
|---|
| Highest positive association |
| Very strong positive association |
| Moderately strong positive association |
| Weak positive association |
| Negative association |

Figure 10: Normalized concentration of trace elements in the rock samples of Mlindi Ring Structure

The samples from Mlindi Ring Structure indicate possible presence of gold and base metals especially zinc, copper and nickel. It should be noted that the XRF model that we used did not have calibrating sample for gold and base metals. As such, the reliability of the results for gold and base metals are less than for whole rock geochemistry and rare earth metals. The occurrences of gold and base metals from the analysis do not associate well with phosphorous in other rocks apart from meta-pyroxenite. Their abundance does not depend on each other in relation to other mineralized elements in Mlindi Ring Structure (Table 3). The most surprise result is the gold concentration in the ring structure that goes up 2 to 74 ppm. Every rock unit in the ring structure indicates presence of gold, which could be a red flag in the results. It should be noted that gold occurs in almost every environment with less association with any rare earth or trace elements. The only association of gold to other mineralized elements in Mlindi Ring Structure is that they both occur in abundance where there is presence of apatite-mineralized meta-pyroxenite (Figures 3 and 4). Gold concentration in Aplite is at 11 ppm, meta-gabbro and micro-syenite at 3 ppm, and quartzofeldspathic and Perthosite at 7 ppm. The higher concentration of gold in Mlindi Ring Structure is therefore associated with meta-pyroxenite. Most of the sampled locations indicated less than 10 ppm of gold and one location showed a considerable 74 ppm for soil sample while the highest for rock sample showed 70 ppm of gold. Zinc concentration is less than 163 ppm with the highest values from the quartzofeldspathic granulite. Aplite and meta-gabbro show lower concentration of zinc.

5.6 Geochemical relationship with apatite mineralization

The meta-pyroxenite hosting apatite is discussed as an indicator of mineralization for rare earth elements. The presence of apatite in these rocks can be used to differentiate the presence and absence of mineralization (e.g. Belousova et al. 2002). This may help to reduce exploration targets for these minerals. Apart from rare earth minerals, the present study also associated the presence of apatite with the possible trace elements mineralization.

Copper concentration is relatively smaller compared to zinc in all the other rock units apart from the meta-pyroxenite. Nickel abundance in the samples goes up to 670 ppm. Rare earth minerals and its associated minerals like Yttrium also form part of the elements in the Mlindi Ring Structure making it a possible multi-commodity deposit. Comparatively, less heavy rare earth minerals were found from the analysis as opposed to light rare earth minerals, which show much higher concentrations. Possibly, using good and powerful analytical instrument and technique, like induced coupled plasma – mass spectrometry (ICP-MS), could produce much better results. The heavy REEs occur in very low abundance of less than 38 ppm. The most abundant rare earth element is Neodymium. It counts up to 1168 ppm. The distribution of rare earth minerals in the different lithologies is not even with the most of it recorded in the meta- pyroxenite. Other rare earth minerals identified include cerium, lanthanum and praseodymium. Most of these rare earths are

concentrated in the meta-pyroxenite environment or other closely associated ultramafic-mafic rocks.

5.7 Relationship between geochemistry and geophysics

The relationship between phosphorous, which is from apatite, and the mineralization in Mlindi Ring Structure was already discussed above (Section 5.4). Phosphorous presence indicates possible mineralization. At depth, this model of relationship can be inferred if we have enough drill-hole data. The presence of magnetic minerals, hence higher susceptibility, correspond to the presence of phosphorous and hence apatite. From the geochemistry point of view, most of the mineralization are confined to meta-pyroxenite. However, not every meta-pyroxenite showed high susceptibility values (Fig 4). This could be that at depth, the magnetic values are less than on the surface. Nevertheless, where the magnetic susceptibility is lower, the phosphorous/apatite concentration seems to be lower as well, and so are the economic minerals. This directly relates the presence of apatite to high magnetic areas in Mlindi Ring Structure. It has also been shown from the geochemical point on view in section 5.4 that presence of other magnetic minerals are in tandem to the mineralization in Mlindi Ring Structure. The rare earth minerals and trace elements are mostly associated with iron, phosphorous and calcium in Mlindi Ring Structure. The higher magnetic anomaly areas correspond to high magnetic minerals which makes it possible to delineate the full extent of mineralization in Mlindi Ring Structure.
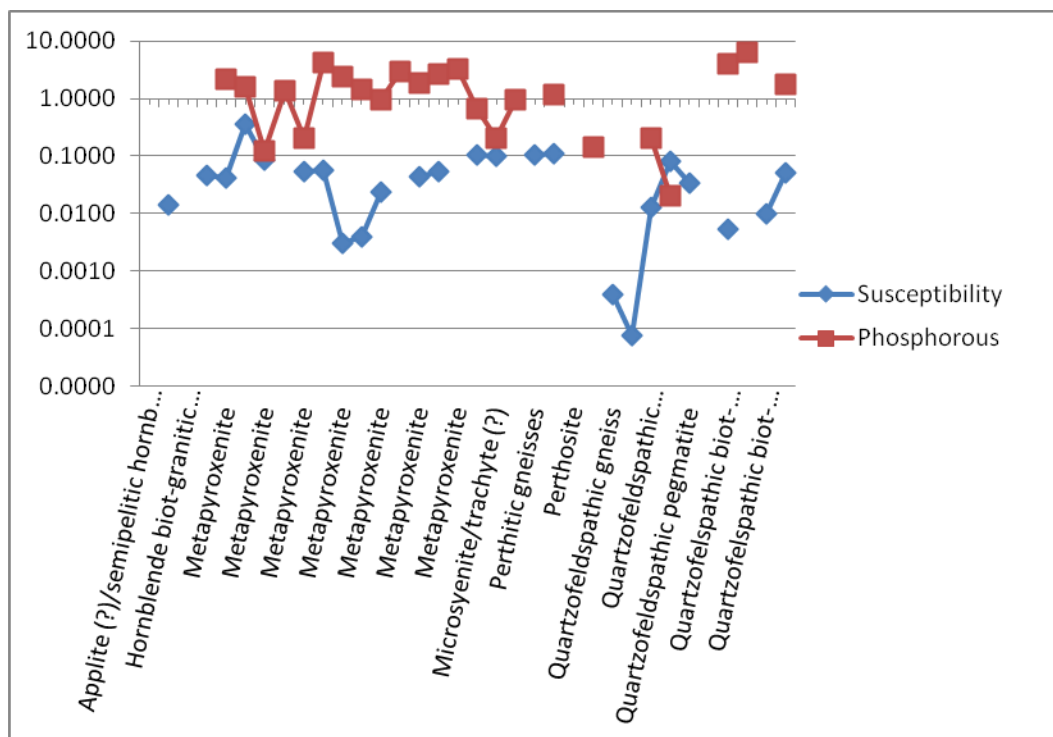
Figure 11: A normalized relationship between calculated magnetic susceptibility on the surface and phosphorous content

6 Conclusions and recommendation

The final interpretation of magnetic susceptibility to apatite relationship was based on the same sample location. Susceptibility was calculated from magnetic data on the surface and on an upward continuation of 100 m, 150 m and 200 m depth. The apparent susceptibility map is based on reduce to pole map. This indicates the full extent of magnetic body in an area. The comparison of magnetic body response and the geologically mapped meta-pyroxenite are not matching. The full extent seems to be bigger on the magnetic data with small non-magnetic rocks in the middle and southern part of the Ring Structure. The geochemical signature of different rock units containing phosphate has been constrained on the magnetic data to understand the full extent of the subsurface mineralization. The calculated magnetic susceptibility and depth estimates of reduce to pole magnetic data has been used in the process.

The combination of geochemical and geophysical analyses of the Mlindi Ring Structure has identified it as a possible multi-commodity deposit. The Mlindi Ring Structure contains considerable amounts of gold, zinc, nickel copper and rare earth elements. The mineralization of gold and base metals is found in almost all the lithologies but very high in

apatite bearing meta-pyroxenite, despite caution on the results for these values. On the other hand, rare earth elements are mostly associated with mafic rocks i.e. meta-gabbro and meta-pyroxenite and less or not at all in silica rich rocks like quartzofeldspathic gneisses. Furthermore, this mineralization is associated with high iron content which makes them easily delineated using magnetic anomaly. The mineralized iron-rich lithologies are estimated to occur from the surface to 150 m depth.

The current results reflect the methodology and the number of samples used for the analysis. However, from a geochemistry standpoint, a more detailed sampling interval for all lithologies and more advanced analytical methods preferably using ICP-MS can possibly improve the results. The geophysical inversion techniques used in this study is used where there is no prior information. However, future inversions should include other geological information for instance, when drilling is done in the area. Other 3D inversion method could also resolve the anomaly better.

Acknowledgement

References

Alva-Valdivia, L. M. *et al.* (2001) 'Rock-magnetism and ore microscopy of the magnetite-apatite ore deposit from Cerro de Mercado, Mexico', *Earth, Planets and Space*, 53(3), pp. 181–192. doi: 10.1186/BF03352375.

Ashley, B. E. 1952a. The Geology of the Neno District. Zomba, Malawi: *Government Printer*.

Ashley, B. E. 1952b. The reconnaissance Geology of the Neno Area, Malawi. Zomba, Malawi: *Government Printer*.

Bates, M. & Mechennef, F. 2013a. Data Acquisition Report: High Resolution Airborne Magnetic and Gravity Survey: The Comprehensive Countrywide Airborne Geophysical Survey. Ottawa, ON Canada.

Bates, M. & Mechennef, F. 2013b. Data Processing Report: High Resolution Airborne Magnetic and Gravity Survey: The Comprehensive Countrywide Airborne Geophysical Survey. Ottawa, ON Canada.

Belousova, E. a. *et al.* 2002. Apatite as an indicator mineral for mineral exploration: Trace-element compositions and their relationship to host rock type', *Journal of Geochemical Exploration*, 76: 45–69. doi: 10.1016/S0375-6742(02)00204-2.

Bloomfield, K., & Garson, M. S. 1965. The geology of the Kirk Range, Lisungwe Valley area. Bulletin No 17. Malawi Geological Survey Library, Zomba, Malawi: *Government Printe*r.

Bloomfield, K. 1957. Report on Fieldwork in the Kirkrange and Zomba Area. Zomba, Malawi: *Government Printer*.

Bloomfield, K. 1959. The Geology of Neno Area. Zomba, Malawi: *Government Printer*.

Bloomfield, K. 1960. Mlindi Ring Structure. Zomba, Malawi: *Government Printer*.

Bloomfield, K. 1965. Infrascrustal Ring-complexes of Southern Malawi. Zomba, Malawi: *Government Printer*.

Broughm, S. G. *et al.* 2017. Mineral chemistry of magnetite from magnetite-apatite mineralization and their host rocks: examples from Kiruna, Sweden, and El Laco, Chile, *Mineralium Deposita*, 52(8): 1223–1244. doi: 10.1007/s00126-017-0718-8.

Carter, G. S. & Bennet, J. D. 1973. *T*he Geology and Mineral Resources of Malawi. Bull. Geol. Surv. Mw, 6. Zomba, Malawi: *Government Printer*.

Chisale, R. T. K. & Kaphwiyo, C. E. 1987. Rock phosphate resources of Malawi - a review, in Wachira, J. K. & Notholt, A. J. G. (eds) *Agrogeology in Africa*. 226th edn. Commonwealth Sci. Council, 77–83.

Clark, D. A. & Emerson, D. W. 1991. Notes on rock magnetization characteristics in applied geophysical studies, *Exploration Geophysics*, 22(3): 547–555. doi: 10.1071/EG991547.

Fleischer, M. 1965. Some aspects of the geochemistry of yttrium and the lanthanides, *Geochimica et Cosmochimica Acta*, 29(7): 755–772. doi: http://dx.doi.org/10.1016/0016-7037(65)90029-3.

Harlov, D. E., Andersson, U. B. & Nystro, J. O. 2002. Apatite – monazite relations in the Kiirunavaara magnetite – apatite ore , northern Sweden, 191: 47–72.

Iddings, J. P. 1898. Chemical and Mineral Relationships in Igneous Rocks, *The Journal of Geology*, 6(11): 951–952.

Innocenzi, V. *et al.* 2014. Yttrium recovery from primary and secondary sources: A review

of main hydrometallurgical processes, *Waste Management*, 34(7): 1237–1250. doi: 10.1016/j.wasman.2014.02.010.

Jachens, R. C. & Blakely, R. J. 1986. A New Isostatic Residual Gravity Map of the Conterminous United States, *Journal of Geophysical Research*, 91(5): 8348–8372.

Kanazawa, Y. & Kamitani, M. 2006. Rare earth minerals and resources in the world, *Journal of Alloys and Compounds*, 408–412: 1339–1343. doi: 10.1016/j.jallcom.2005.04.033.

Laval, M. & Hottin, A. M. 1992. The Mlindi ring structure. An example of an ultrapotassic pyroxenite to syenite differentiated complex, *Geologische Rundschau*, 81(3): 737–757. doi: 10.1007/BF01791389.

Lee, M., Morris, B., & Ugalde, H. 2010. Effect of signal amplitude on magnetic depth estimations. *Leading Edge (Tulsa, OK)*, *29*(6): 672–677. https://doi.org/10.1190/1.3447778

Letros, S. W., Strangway, D. W. & Geissman, J. 1983: Apparent susceptibility mapping in the Kirkland Lake area, Ontario, Abitibi greenstone belt, Canada, *Journal of Earth Science*, 20: 548–560.

Li, J. & Morozov, I. 2007. Geophysical Investigations of the Precambrian Basement of the Williston Basin in south-eastern Saskatchewan and south-western Manitoba', *University of Saskatchwan*.

Morel, S. 1958. The Geology of the Middle Shire Area., *Bull. Geol. Surv. Mw, 10.* Zomba, Malawi: *Government Printer*.

Mushayandebvu, M. F. *et al.* 2004. Grid Euler deconvolution with constraints for 2D structures', *Geophysics*, 69(2): 489–496. doi: 10.1190/1.1707069.

Ranganai, R. T. & Ebinger, C. J. 2008. Aeromagnetic and Landsat TM structural interpretation for identifying regional groundwater exploration targets, south-central Zimbabwe Craton, *Journal of Applied Geophysics*, 65(2): 73–83. doi: 10.1016/j.jappgeo.2008.05.009.

Reid, A. B. *et al.* 1990. Magnetic interpretation in three dimensions using Euler deconvolution', *Geophysics*, 55(1): 80–91. doi: 10.1190/1.1442774.

Sadek, H. S., Rashad, S. M., & Blank, H. R. 1984. *Spectral analysis of aeromagnetic profiles for depth estimation principles, software, and practical application.* Department of the interior U.S. *geological survey.*

Wang, W., Pranolo, Y. & Cheng, C. Y. 2011. Metallurgical processes for scandium recovery from various resources: A review', *Hydrometallurgy*, 108(1–2):100–108. doi: 10.1016/j.hydromet.2011.03.001.